https://doi.org/10.5194/cp-2022-40
Preprint. Discussion started: 13 May 2022

Climate of the Past
Discussions

Response of terrigenous weathering to the African monsoon during the penultimate deglaciation and the last interglacial period

Christopher J. Lepre[1], Clara Chang[2], Owen Yazzie[3]
[1]School of Earth, Environment & Society, Bowling Green State University, Bowling Green OH, 43403, USA
[2]Lamont-Doherty Earth Observatory, Columbia University, Palisades, NY, 10964, USA
[3]BS program in Geological Sciences, Arizona State University, Tempe, AZ, 85287 USA
Correspondence to: Christopher J. Lepre (leprecj@bgsu.edu)

Abstract. Climates of the last interglacial period (i.e., marine isotope stage 5e; MIS 5e) were associated with hydrographic, ecological, and human expansions across northern Africa. Model simulations and geological proxy data for northern subtropical latitudes resolve a dry penultimate deglaciation (Heinrich stadial 11; HS11) followed by an abrupt increase of African rainfall that predates the orbital insolation maximum of early MIS 5e. These climate changes have been attributed to the equatorward displacement and rebound of the tropical rainbelt in response to glacial reorganizations of Atlantic meridional overturning circulation (AMOC). In this paper, we examine MIS 5e and HS11 paleoenvironments by using X-ray fluorescence measurements to construct a Rb/Sr proxy record of terrigenous delivery to marine core site VM 30-40 (0º 12’ S, 20º 09’ W, 3,706 m depth) of the Atlantic Ocean. The geochemical timeseries was inferred to represent continental weathering influenced by the African monsoon evolving over the last ~260 kyr of the Quaternary. Peak Rb/Sr values were observed at the most recent and penultimate glacial maxima, attributed to different modes of continental weathering or perhaps dissolution of Sr-bearing phases by corrosive deep waters. Spectral coherency results and filtering of the Rb/Sr timeseries demonstrate an absence of obliquity yet a predominance of a precession signal that shares the best phase relationships with March-April-May insolation at the equator. This vernal signal is interpreted to indicate that the terrigenous fraction of the core had low-latitude source areas, where the monsoonal cycle is most sensitive to insolation changes about the equinoxes. These data also show a wet climate during HS11 that progresses towards peak conditions at ~127 ka, nearly coinciding with the insolation maximum of early MIS 5e. We interpret that latitude plays an important role in determining the outcomes of AMOC forcing, with the low-latitude terrigenous sources differing from the northern subtropics because the former was into the (equatorward) direction of rainbelt displacement. Lastly, these results suggest a very limited role for obliquity-controlled paleoenvironmental changes within Middle Stone Age habitats and may support previous interpretations that social networks were enhanced between the west and north African regions during times of increased rainfall forced by precession-modulated insolation.

1. Introduction

Terrigenous material transported through Earth's atmosphere influences global biogeochemical cycles, climate conditions, and public health (Prospero et al., 2002). The largest source of this material is the dust particles that emanate from drylands of North Africa and carried aloft by monsoonal winds and related aeolian systems (**Fig. 1**). A major constituent of dust is weathering products of sediments and soils (Maher et al., 2010). This is readily inferred from the colors of West African dust plumes that carry hematite and goethite derived from the regolith (Formenti et al., 2014; Moskowitz et al., 2016; Oldfield et al., 2014). Studying the conditions under which this dust is produced and transported helps to understand the potential response of African landscapes to vegetation changes and erosion caused by future climates (de Menocal, 2015; McGee et al., 2013; Yuan et al., 2020). To study these relationships, geological research has focused on the last interglacial period represented by MIS 5e that lasted from about 129-116 ka (Govin et al., 2015). This interval is characterized by low global ice volume and high sea level, thus providing many proxy records for studying the Earth system under a global warming scenario (Kukla et al., 2002). During MIS 5e, regions of northern Africa were transformed into verdant landscapes associated with enhanced boreal summer insolation (Blanchet et al., 2021; Dupont, 2011; Hooghiemstra et al., 2006). However, there is still much debate about what controls African climate change and the timing/rate of the response to the forcing (Bosmans et al., 2015; Menviel et al., 2021; Shanahan et al., 2015).

Marine core records collected off of the West African continental margin provide information for interpreting the paleoclimate context of prehistoric humans. Some hypotheses use these records to suggest that high-latitude glacial cycles driven by obliquity caused cooling and drying effects that impacted major juncture of human origins in Africa (deMenocal, 2004). Contrastingly, low-latitude changes in coupled ocean-atmosphere systems may have been stronger drivers of environmental change within human habitats (Berner et al., 2022; Kaboth-Bahr et al., 2021; Lepre and Quinn, 2022; Trauth et al., 2021; van der Lubbe et al., 2021). Recent West African archaeological work has produced a time-constrained sequence of the Middle Stone Age (MSA) through the last two glacial-interglacial cycles, yet the connections between lithic culture variability and paleoclimate are not well understood (Allsworth-Jones, 2021; Chevrier et al., 2018; Douze et al., 2021; Lespez et al., 2008). Study of West African marine core records during the last interglacial period (Castaneda et al., 2009) suggests that increased rainfall and vegetation may have facilitated the interconnectivity of north African social groups (Drake et al., 2011). Such favorable conditions predictably recurred through the late Quaternary as a consequence of insolation forcing of monsoonal intensities (Grant et al., 2022). However, marine core dust records have been questioned as a

https://doi.org/10.5194/cp-2022-40
Preprint. Discussion started: 13 May 2022

Climate of the Past
Discussions

viable dataset for investigating links between climate and human prehistory of West Africa (Skonieczny et al., 2019). Marine dissolution events during glacial epochs, independent of African climate, have been recognized throughout the Atlantic Ocean (Verardo and Mcintyre, 1994). These events may have imparted the marine core sediments with spurious evidence of obliquity-driven changes to the monsoon (Skonieczny et al., 2019).

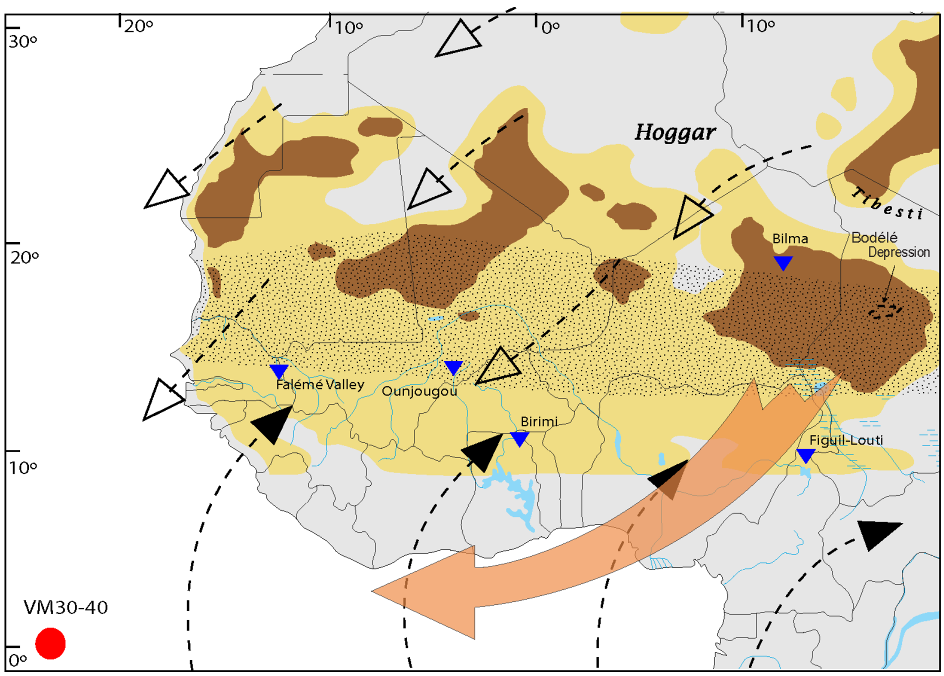

Figure 1: Map of northwestern Africa showing the location of the studied VM 30-40 marine core and archaeological, meteorological, and physiographic features discussed in the text. Archaeological localities shown as blue inverted triangles (Chevrier et al., 2018). Open arrows indicate trade winds, closed arrows are monsoonal, and large arrow is Harmattan (Trauth et al., 2009). Dust sources indicated in brown and yellow (Muhs et al., 2014; Prospero et al., 2002). Approximate position of the Sahel denoted by stippled area (Nicholson, 2018).

To address these issues, we examined the most recent ~260 kyr of the Quaternary that is recorded by eastern equatorial Atlantic marine core VM 30-40 (see **Fig. 1** for location). We selected this core in particularly because it has a well-resolved marine isotope stage (MIS) record and oxygen-isotope age calibration (McIntyre et al., 1989) and provides a record of precession climate forcing of freshwater lacustrine diatom deposition (Pokras and Mix, 1987). However, there has been little study of other type terrigenous materials in the core (Balsam et al., 1995; Rowland et al., 2021). We developed a new X-ray fluorescence (XRF) record for VM 30-40 to sample a variety of sediment and soil environments different

https://doi.org/10.5194/cp-2022-40
Preprint. Discussion started: 13 May 2022

from the lacustrine diatom facies. Rb/Sr measurements on the core (**Fig. 2**) were used to provide a proxy record of continental weathering (Hemming, 2007). Comparisons with other marine core sediments from the West Africa margin and model simulations (Govin et al., 2014; Menviel et al., 2021) are made to infer different controls of terrigenous production and transport over the late Quaternary. Finally, we use the collected data to suggest a paleoclimate context for MSA West African archaeological sites.

2. Materials and methods

2.1. Stratigraphy and setting of VEMA core 30-40

In this paper, we focus on and provide new data for VEMA core 30-40 (VM 30-40, IGSN number DSR000ZD0). This core was initially split and described in the 1970s and has been housed at the Lamont-Doherty Core Repository. It was obtained from eastern equatorial Atlantic waters (0º 12' S, 20º 09' W) at a depth of 3706 m (**Fig. 1**). Prior stratigraphic analysis of VM 30-40 (**Fig. 2**) indicates that the recovered sediment record is 755 cm long, representing the last ~256.7 kyr to MIS 7, with a mean sediment accumulation rate of 1 cm per 340 years (Imbrie et al., 1984; McIntyre et al., 1989).

VM 30-40 has the typical sediments of the marine cores of the eastern tropical Atlantic that are dominated by biogenic $CaCO_3$ and a subordinate amount of terrigenous detritus (Bozzano et al., 2002; Bradtmiller et al., 2007; Moreno et al., 2001; Rowland et al., 2021; Skonieczny et al., 2019; Tiedemann et al., 1994). Core records also contain minor fractions of biogenic opal, phytoliths, and may preserve pollen (deMenocal et al., 1993; Hooghiemstra et al., 2006; Leroy and Dupont, 1994; Lézine and Casanova, 1991). Previously, VM 30-40 has been used for paleoceanographic and paleoclimate research, studied for diatoms, phytoliths, $CaCO_3$, color/iron-oxide content, isotopes, and thorium-normalized dust concentrations (Balsam et al., 1995; Bradtmiller et al., 2007; Imbrie et al., 1984; McIntyre et al., 1989; Pokras, 1987; Rowland et al., 2021).

VM 30-40 was retrieved at about 1400 km SW from the coast of West Africa and the site lies at the southern part of the winter dust plume (Pokras and Mix, 1985). Input from the seasonal plumes to the marine core sites affords high-resolution paleoclimate records of continental conditions (Adkins et al.,

https://doi.org/10.5194/cp-2022-40
Preprint. Discussion started: 13 May 2022

2006; McGee et al., 2013; Mulitza et al., 2010; Palchan and Torfstein, 2019; Trauth et al., 2009).

Figure 2: Stratigraphic information for VM 30-40 marine core. Black dots indicate MIS positions and dates listed in Table 1. Lithological symbols: (1) interbedded layers of foraminiferal ooze and foraminiferal marl ooze, (2) foraminiferal marl, (3) foraminiferal ooze, and (4) foraminiferal marl ooze. Lithostratigraphic description from https://www.ngdc.noaa.gov/mgg/curator/data/vema/vm30/040/. Oxygen isotope data retrieved from https://doi.org/10.1594/PANGAEA.56361. Dashed box denotes the interval pictured in Fig. 3.

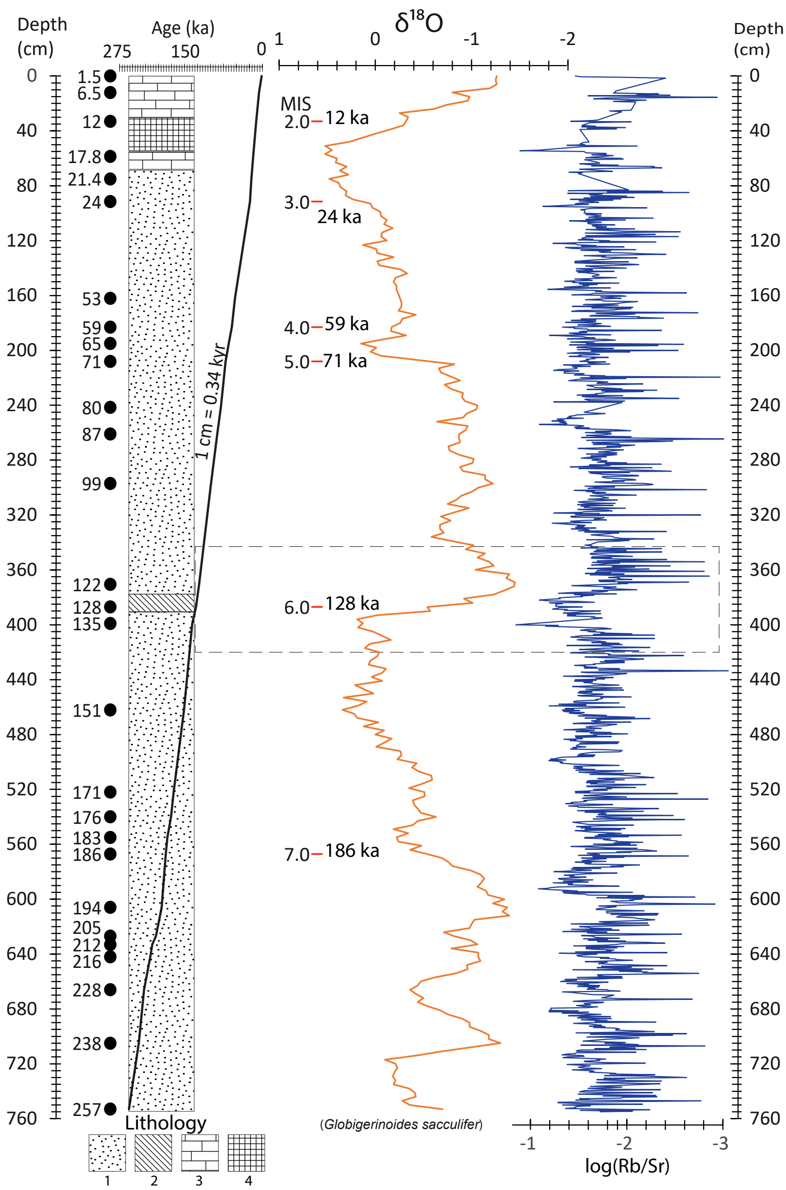

Winter dust plumes are carried by the trade winds as they move through the Sahara-Sahel region (Schwanghart and Schütt, 2008). The position of the trade winds follows the migration of the Intertropical Convergence Zone (ITCZ) in response to the seasonal location of maximum insolation across the African landmass. Through the summer-winter transition in the Northern Hemisphere, the ITCZ migrates towards the equator and the trade winds follow south to generate the winter dust plume at 10-20º N (Prospero et al., 2014).

There are several potential source areas that may contribute to the dust plumes (Heinrich et al., 2021; Jewell et al., 2021; Moreno et al., 2006; Oldfield et al., 2014; Scheuvens et al., 2013; Stuut, 2005). One of the more important sources is thought to be the Bodélé Depression (Washington et al., 2006), effectively the footprint of the now-exposed lake beds for mega-Lake Chad (Armitage et al., 2015). Lacustrine deposits of the Bodélé Depression are suggested to be high-yielding sources not only for the plumes but also for the Earth's global dust budget (Maher et al., 2010; Moskowitz et al., 2016; Prospero et al., 2014, 2002; Washington et al., 2006). Lacustrine freshwater diatoms are present within VM 30-40 but a specific geographic provenance on the continent is uncertain (Pokras, 1987; Pokras and Mix, 1987, 1985).

2.2. XRF measurements

Before the scanning of core VM 30-40, the surfaces of its sections were scraped clean as standard protocol. The core sections were scanned lengthwise along the center of the core surface using an Itrax Core Scanner (Cox Analytical Systems, Mölndal, Sweden) at the Lamont-Doherty Earth Observatory. Analyses were performed using settings of 30 kV and 30 mA with a Mo tube, a step size of 5mm and an exposure time of 5 seconds. The XRF data were collected in total counts (Croudace and Rothwell, 2010) and we transformed the Rb and Sr data by calculating the log-ratios of the element intensities. Log-ratios have been shown to be simple linear functions of log-ratios of concentrations that minimize biases introduced by analytical conditions of XRF measurements (Hodell et al., 2015; Weltje and Tjallingii, 2008). We use the ratio between Rb and Sr to interpret weathering, and infer terrigenous deposition and paleoclimate change (Hemming, 2007). Rb/Sr ratios in West African marine core sequences have been used as proxy indictors of continental weathering rates and late Quaternary paleoclimate (Cole et al., 2009).

https://doi.org/10.5194/cp-2022-40
Preprint. Discussion started: 13 May 2022

Sr-bearing phases tend to break down early on and Rb is retained in K-rich mineral phases (White et al., 2001). Within monsoon soils, the variations in the Rb/Sr ratio may be controlled by the relative durability of the K-bearing materials and the amount of strontium loss during weathering (Chen et al., 1999).

Table 1: VM 30-40 core chronology*

MIS substage‡	Age (ka)	Depth (cm)
nr	1.5	0
1.1	6.5	12
2.0	12	33
2.22	17.8	58.5
2.24	21.4	75
3.0	24	91.5
3.3	53	162
4.0	59	183
4.2	65	195
5.0	71	208
5.1	80	241.5
5.2	87	261
5.3	99	297
5.5	122	370.5
6.0	128	387
6.2	135	399
6.4	151	462
6.5	171	522
nr	176	540
6.6	183	555
7.0	186	567
7.1	194	606
7.2	205	627
nr	212	633
7.3	216	642
7.4	228	666
7.5	238	705
nr	257	753

* based on the SPECMAP oxygen isotope age model (McIntyre et al., 1989)

‡nr = not reported

2.3. Interpreting paleoclimate data from the XRF measurements

We constrain the terrigenous fraction that accumulated during HS11 and the early part of MIS 5e with the established $d^{18}O$ record of the core between 370 and 400 cm (**Fig. 2**). Depth positions of MIS datums

https://doi.org/10.5194/cp-2022-40
Preprint. Discussion started: 13 May 2022

6.2 (135 ka), 6.0 (128 ka), and 5.5 (122 ka) were used to construct a linear regression age model and scale the log(Rb/Sr) depth series to time. The log(Rb/Sr) timeseries for the HS11 to early MIS 5e interval was then compared directly to the astronomical solution of insolation at 23° N for boreal summer (**Fig. 3**). Other intervals of the log(Rb/Sr) timeseries were calibrated using the mean sedimentation rate of 1 cm per 340 years (**Fig. 2**). The core's $d^{18}O$ record is from the planktonic foraminifera *Globigerinoides sacculifer* (Imbrie et al., 1984) and the data reported in Table B1 of McIntyre et al. (McIntyre et al., 1989) provides 28 core depths matched to 28 dates based on the SPECMAP oxygen isotope stratigraphy and marine isotope stages (**Fig. 2** and **Table 1**).

Pokras and Mix (Pokras and Mix, 1987) resolved a record of climatic precession and its harmonics from the spectral analysis of the freshwater lacustrine diatoms preserved in VM 30-40. Eolian-transported diatoms in marine sediment cores of West Africa derive from the deflation of diatomaceous deposits in dry North African lake beds (deMenocal et al., 1993). Thus, the diatom increases within marine core sequences are traditionally thought of as indirect indicators of lake levels and aridity. Pokras and Mix (Pokras and Mix, 1987, 1985) interpreted that major peaks in the VM 30-40 diatom record correlated to the early phases of insolation minima for boreal summer (**Appendix Fig. A1**); however, these authors also noted that diatom maxima were approximately in phase with spring insolation minima (**Appendix Fig. A1**) .

To assess if other components of the terrigenous fraction carry orbital forcing, the log(Rb/Sr) depth (cm) series was scaled to time by using the core's overall sedimentation rate of 1 cm = 0.34 kyr and then resampled to every 0.17 kyr, which was the median/mean sample interval (0.5 cm) of XRF measurements. We then treated the log(Rb/Sr) timeseries to coherency analysis with the *AnalySeries* software (Paillard et al., 1996). Spectral coherency comparisons were made with eccentricity-tilt-precession (ETP) (Laskar et al., 2004) and the astronomical solution of ETP was generated with *Acycle* software (Li et al., 2019). The Blackman–Tukey cross spectrum method was used with a Bartlett window and zero-coherency set to 0.5 (80%) level of significance.

3. Results and interpretations

3.1. Variations in Rb/Sr ratios

https://doi.org/10.5194/cp-2022-40
Preprint. Discussion started: 13 May 2022

Climate of the Past
Discussions

The log(Rb/Sr) ratios reveal no long-term directional trends over the last ~257 kyr; however, recurring through the timeseries are evident cycles with durations of 1000s and 10,000s years (**Fig. 2**). The two largest values of the log(Rb/Sr) timeseries are observed at about 135 ka and 18 ka. These approximately correlate with glacial maxima of MIS 6 and 2, respectively (**Fig. 2**). Most studies suggest that potential West African dust sources were arid during MIS 6 and 2 (Gasse, 2000; Kim et al., 2008; Menviel et al., 2021). Therefore, the chronostratigraphy suggests that the largest values of log(Rb/Sr) correlate with two substantially dry phases of the North African monsoon over the last ~150 kyr. Cole et al. (Cole et al., 2009) also studied Rb/Sr ratios in marine core sediments of West Africa and found larger Rb/Sr ratios at the glacial maximum of MIS 2 as compared to the early-middle Holocene African Humid Period (AHP). These authors and others (Cole et al., 2009; Jung et al., 2004) explained the differences by inferring that the Rb/Sr ratios during glacial aridity is controlled by less water available for hydrolysis and a predominance of physical over chemical weathering. During MIS 2 aridity, alkaline mineral deposits were generated when North African soils and lakes desiccated (Gasse, 2000). Under such dryness, the precipitation of caliches and evaporites causes Ca- and Na-rich minerals to become sequestered into deflation-resistant horizons (Mabbutt, 1977). This may decrease the amount of Sr-bearing minerals available for aeolian mobilization and transport, increasing the Rb/Sr ratios of the dust plumes. Alternatively, high Rb/Sr ratios at glacial epochs may indicate that in-situ dissolution has affected the terrigenous carbonate fraction of the marine sediments. During glacial epochs, deep ocean circulation changes bring corrosive Antarctic Bottom Water to near West African margin (Bozzano et al., 2002; Skonieczny et al., 2019). This may have removed some of the Sr carried by the terrigenous Ca-bearing fraction.

Rb/Sr ratios may increase with increasing continental weathering (Hemming, 2007). An increase in continental weathering is typically associated with the available moisture and thus wetter climates (Kelly et al., 1998). Under wet monsoon conditions, soils may become enriched in Rb through weathering processes that remove “softer” minerals that bear Sr (Chen et al., 1999). In African environments, the distribution of Rb and Sr is link to a number of interrelated factors of mineral substrate, geological setting, and hydroclimate (Cole et al., 2009; Janzen et al., 2020; Jewell et al., 2021; Jung et al., 2004; Moreno et al., 2006). Sr commonly infiltrates into many types of geologic and biotic systems because it easily substitutes for Ca or Na due to their similar ionic radii (Blum and Erel, 1997; Koch et al., 1992). Mineral phases that

https://doi.org/10.5194/cp-2022-40
Preprint. Discussion started: 13 May 2022

Climate of the Past
Discussions
Open Access
EGU

carry Sr are soluble carbonates/sulfates or unstable plagioclase. In comparison, K-rich micas and feldspars are less reactive and tend to be retained within soils and saprolites during weathering (Blum et al., 1994; White et al., 2001). Rb substitutes for K and is thus associated with the more stable mineral phases (Blum and Erel, 1997).

Figure 3: Paleoenvironmental information for the penultimate deglaciation and interglacial. The resolved log(Rb/Sr) variations for marine core VM 30-40 (this study) plotted with June solstice insolation at 23° N indicated by red dashed line. Note ~2 kyr interval of no data. Stable oxygen isotope data for VM 30-40 from https://doi.org/10.1594/PANGAEA.56361. Horizonal dashed line across the log(Rb/Sr) graph is placed to guide the eye towards values greater than -1.5. Position of the MIS 5e interval after Govin et al. (Govin et al., 2015).

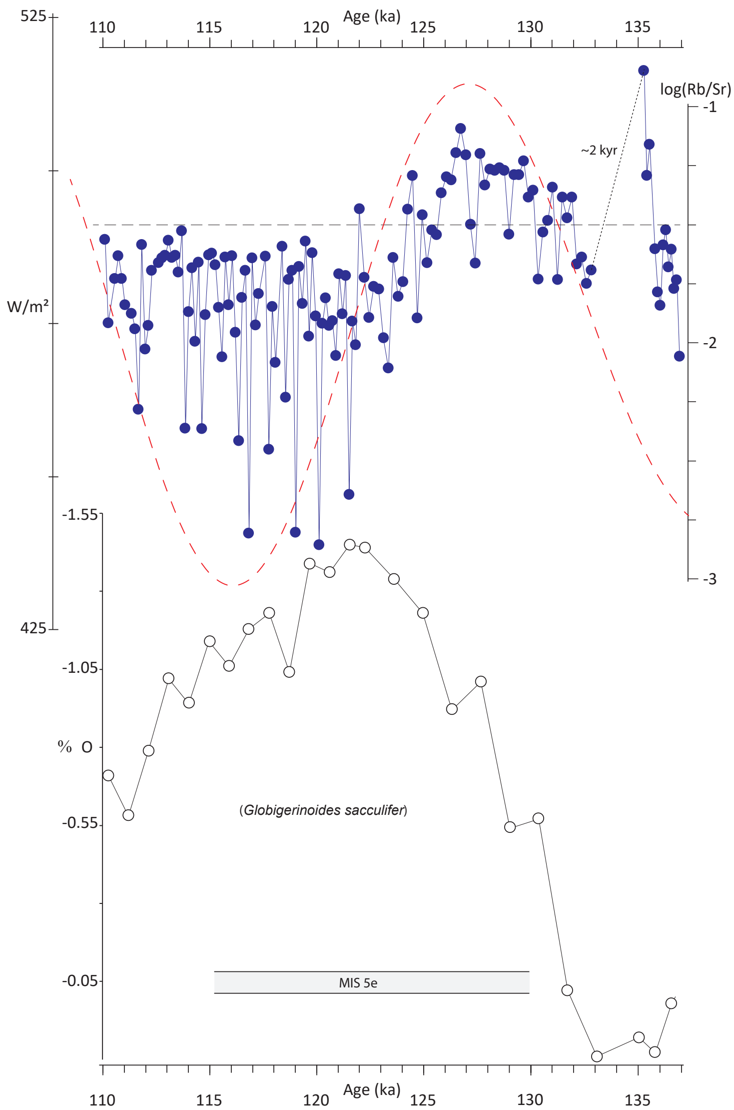

3.2. The last deglaciation and interglacial period

During MIS 5e, log(Rb/Sr) variations are close to being in phase with summer insolation variations at 23° N (**Fig. 3**). Following the penultimate glacial maximum at ~135 ka, the VM 30-40 core demonstrates increasing log(Rb/Sr) values during HS11. The small yet initial increase occurs over a ~1000 yr interval from about 133-132 ka (**Fig. 3**) and the log(Rb/Sr) values suggest that peak interglacial conditions were attained by ~127 ka, nearly coincident with the timing of the summer insolation maximum at 23° N. After ~127 ka the terrigenous record indicates a trend of decreasing values that follow declining insolation (**Fig. 3**). This decreasing trend is interrupted by two brief returns to humidity/warmth, one constrained to 125-124 ka and the second at 122 ka. Drier climates are indicated by comparatively smaller log (Rb/Sr) values between 122-110 ka coincident with low insolation.

3.3. Spectral analysis of orbital climate forcing

Blackman-Tukey coherency results for the log(Rb/Sr) timeseries compared against ETP (**Fig. 4A**) show significant frequencies approximating climatic precession (~20 kyr) . These data also indicate the presence of eccentricity (~100 kyr); however, the chronostratigraphy of VM 30-40 (~0-257 ka) may be too brief for attaching significance to low-frequency cycles. The coherency spectra (**Fig. 4A**) also has significance at ~54 kyr, which is an obliquity harmonic (Zeeden et al., 2019). Another obliquity harmonic might be represented by a small peak at ~28 kyr but it does not achieve the 0.5 (80%) statistical significance. To explore these possible obliquity indications, we conducted spectral coherency analysis of the log(Rb/Sr) timeseries in comparison to the astronomical solution of obliquity (Laskar et al., 2004), the LR04 stack (Lisiecki and Raymo, 2005), and high-latitude (65° N) summer insolation (Laskar et al., 2004). The ~28 kyr period is significant only with obliquity, and the ~54 kyr period has evident significance with the comparisons of obliquity and high-latitude insolation (**Fig. 4B**). These results suggest an absence of the main period of obliquity (~41 kyr) within the log(Rb/Sr) timeseries.

https://doi.org/10.5194/cp-2022-40
Preprint. Discussion started: 13 May 2022

Climate of the Past
Discussions

Figure 4: Blackman-Tukey spectral analysis of geochemical and lithological data from marine core VM 30-40 over the interval of 0-260 ka. Indicated are the positions of eccentricity (100 kyr), obliquity harmonics (54 and 28 kyr) and precession (23 and 18 kyr). (A) Cross-coherency results for log(RB/Sr) compared to ETP. (B) Result for log(RB/Sr) compared to oxygen isotope benthic stack (LR04), June insolation at 65° N (65N), and obliquity (Obl). (C) $CaCO_3$ concentrations of VM 30-40 (from https://doi.org/10.1594/PANGAEA.51365) compared to ETP.

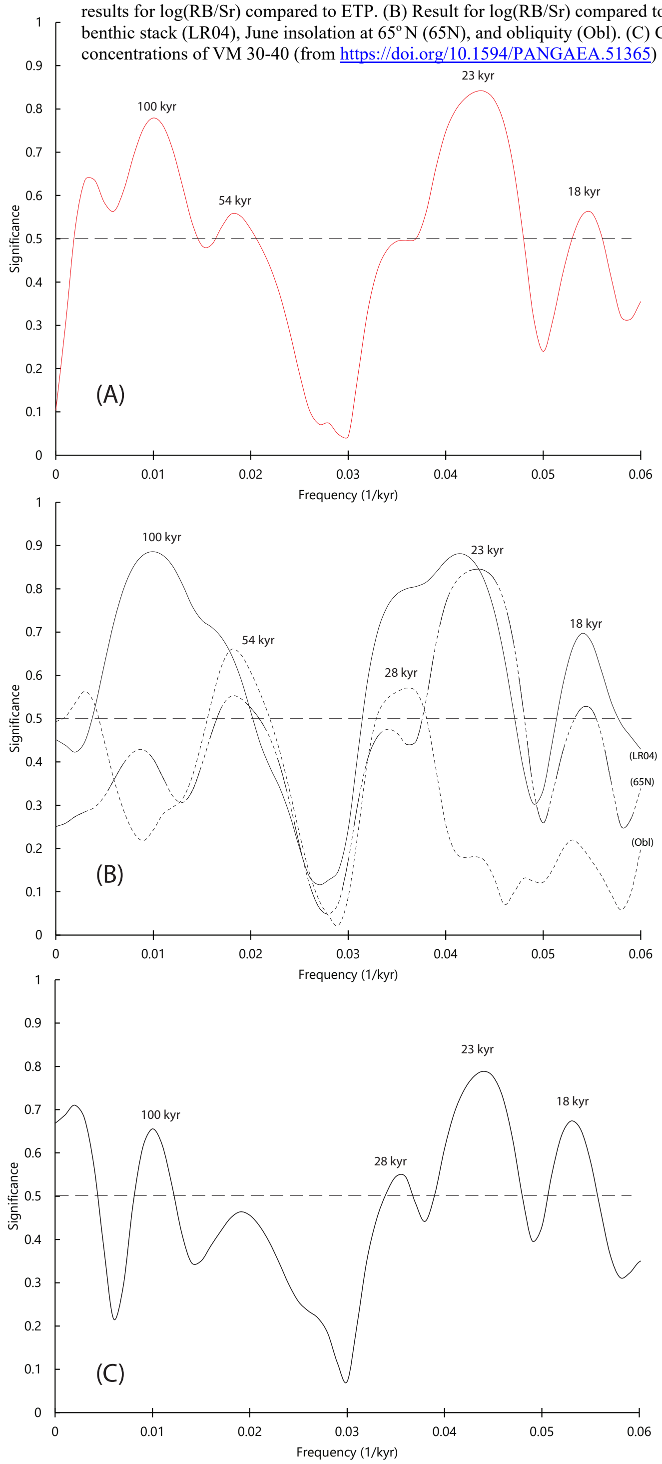

https://doi.org/10.5194/cp-2022-40
Preprint. Discussion started: 13 May 2022

Spectral analysis of the log(Rb/Sr) time series with EPT indicates significant cross-coherency frequencies of ~0.044 (k = 0.84) and 0.055 (k = 0.56) that we correlate with climatic precession cycles of 23 and 18 kyr, respectively (**Fig. 4A**). Precession is an important orbital control on insolation budgets of the tropics (Clement et al., 2004). It determines the timing and position of the seasons within the elliptical path of Earth's orbit (Berger and Loutre, 1997). Most rainfall over the northern West African tropics is derived from summer monsoonal winds that advect Atlantic Ocean moisture to the continent (Nicholson, 2018). When precession places the summer solstice at perihelion, a smaller Earth-Sun distance is coupled to summer insolation (Short and Mengel, 1986), resulting in an associated increase of sensible heating of the African landmass that drives the deep tropical convergence of the monsoon (Kutzbach and Liu, 1997). This is thought to result in wetter summer monsoon seasons for North Africa every ~20 kyr (Grant et al., 2022; Rossignol-Strick, 1985).

4. Discussion

4.1. Orbital climate forcing of the terrigenous record

The presence of an obliquity signal within northern African paleoclimate records of the Quaternary is well documented by studies of marine core sediments near the West African margin (Bloemendal et al., 1988; Bloemendal and deMenocal, 1989). Similarly, eastern Mediterranean sapropel-bearing sequences indicate that North African paleoclimate has had an obliquity component that persists back to before the Plio-Pleistocene intensification of Northern Hemisphere glaciation (Lourens et al., 1996). Some research has suggested that the obliquity signal in these records may derive from low latitude insolation budgets rather than glacial forcing (de Boer et al., 2020; Tuenter et al., 2003). Model simulations suggest that obliquity signals in low-latitude paleoclimate records of Africa may be generated by the cross-equatorial insolation gradient (Bosmans et al., 2015) which also has an effect on the intensity of the winter Hadley cells (Mantsis et al., 2014). These winds are notable for VM 30-40 because the winter plumes carried by the northeast trade winds are thought to contribute dust to this marine site (Pokras and Mix, 1985).

Obliquity signals within the dust records of marine cores from the West African margin have recently been described as spurious evidence of a high-latitude glacial forcing of the North African monsoon (Skonieczny et al., 2019). African dust studies from marine core records (Adkins et al., 2006; Tisserand et al., 2009) measure the concentrations of terrigenous material relative to carbonate ($CaCO_3$). In-situ carbonate dissolution may impart the marine sediment with a glacial-interglacial signal (Bozzano et al., 2002). VM 30-40 isotopic data demonstrate $d^{18}O_{ben}$ enrichment and $d^{13}C_{ben}$ depleted waters for the LGM (Oppo and Fairbanks, 1987; Sarnthein et al., 1994). This may suggest that eastern tropical Atlantic near VM 30-40 was intruded by corrosive deep water at MIS 2 (Skonieczny et al., 2019). However, the results of spectral analyses suggest that few if any of the variations recorded by the log(Rb/Sr) timeseries are attributable to glacial-obliquity forcing (**Fig. 4A and B**). Farthermore, we conducted spectral coherency analysis of the $CaCO_3$ [%] from VM 30-40 using EPT. The results indicate a precession signal at 23 kyr and 18 kyr frequencies, yet the main period of obliquity (~41 kyr) is absent (**Fig. 4C**).

Pokras and Mix's study of VM 30-40 (Pokras and Mix, 1987) interpreted that the lacustrine diatom peaks of the core and thus increased aridity were approximately in phase with spring insolation minima (**Appendix Fig. A1**). However, instead of correlating the two directly, the authors used a nonlinear diagrammatic model to explain how diatom peaks originated from rapid deflation of dust sources in response to the earliest part of summer insolation minima (**Appendix Fig. A1**). Our focused analysis of the MIS 5e interval (**Fig. 3**) suggests that the log(Rb/Sr) values of VM 30-40 are being forcing at least in part by summer insolation, as the largest values rise to the insolation maximum at ~127 ka. To explore these patterns, the precession signal was filtered from the entire log(Rb/Sr) timeseries and directly compared against summer (June, July, August) insolation at 23° N and spring (March, April, May) insolation at the equator. We selected these latitudes because of the strong climate effects received from variations in summer and spring insolation (Berger et al., 2006; Prell and Kutzbach, 1987). The log(Rb/Sr) timeseries has a much better phase relationship with spring insolation (**Fig. 5A**) as compared to summer (**Fig. 5B**).

A spring insolation component to the log(Rb/Sr) timeseries is unexpected given the greatest contrasts of the West African monsoon are at the solstices (Nicholson, 2018). The ITCZ over Africa migrates northward from winter to spring to summer and progressively displaces the northeast trade winds towards subtropical latitudes (Sultan and Janicot, 2003). In autumn, the ITCZ moves south and the trade winds settle over ~20-10° N to generate dust plumes that peak in the winter months (Prospero et al., 2002). The VM 30-40 core site of the eastern equatorial Atlantic is thought to receive terrigenous input mostly from the winter dust plumes (Pokras and Mix, 1985). However, it has been shown that significantly large

https://doi.org/10.5194/cp-2022-40
Preprint. Discussion started: 13 May 2022

amounts of West African dust is transported across the Atlantic during the springtime (Barkley et al., 2019; Prospero et al., 1981). March and April deposition of dust in South American originates from fast-traveling West African plumes, on the order of days, that are initially carried aloft by the Sahara Air Layer (Prospero et al., 2020, 2014). Back trajectories suggest that the dust takes a transatlantic equatorial path emanating from low-latitude African sources (Swap et al., 1992) but also from a wider region in West Africa including the Sahel and the southern Sahara (Prospero et al., 2020).

Bozzano et al. (Bozzano et al., 2002) has suggested that efficient dust uplift and injection into the troposphere occurs just before the onset of rainy seasons. These authors argued that greater precession insolation exacerbates dust mobilization by increasing the storminess and turbulence at the monsoon-trade wind front. Possible vernal locations for this to occur is the onset of the April rainy season along the Guinean Coast (Janicot et al., 2011) and the beginning of the May rainy season over Sudano–Sahelian areas (Sultan and Janicot, 2003).

4.2. Paleoclimate during MIS 5e and HS11

Insolation-driven monsoonal simulations coupled to an Al/Si proxy record of terrigenous runoff have provided a high-resolution reconstruction for northern African climate during the last interglacial (**Fig. 6**).These studies reported an abrupt increase in precipitation at 128.4 to 127 ka associated with an interval of wet conditions that lasted until ~124 ka (Menviel et al., 2021). After which, the climate experienced a gradual drying through the later part of MIS 5e. The log(Rb/Sr) values of VM 30-40 generally agree with the interpretation of a wetter climate at 128-124 ka, in addition to progressive drying from 127 to 120 ka (**Fig. 6**). Significantly different, however, the log(Rb/Sr) timeseries does not reveal the drought-like climate during Heinrich stadial 11 (HS11) (Govin et al., 2014). These very dry conditions terminate at the afore mentioned abrupt increase of precipitation at the end of HS11, with maximum rainfall reached at ~128.4 ka during the early part of MIS 5e (Menviel et al., 2021). Because the abrupt rainfall increase predates the summer insolation maximum by almost 1400 years, it was attributed to Northern Hemisphere deglaciation effects on AMOC that causes ocean-atmosphere feedbacks over northern Africa (Menviel et al., 2021). The log(Rb/Sr) timeseries lacks both the dry conditions and abrupt increase, and instead suggests a progressive

https://doi.org/10.5194/cp-2022-40
Preprint. Discussion started: 13 May 2022

Climate of the Past
Discussions
Open Access
EGU

315 increase in rainfall end of HS11 to early MIS 5e that appears to follow rising insolation to its maximum at

316 ~127 ka (**Fig. 6**).

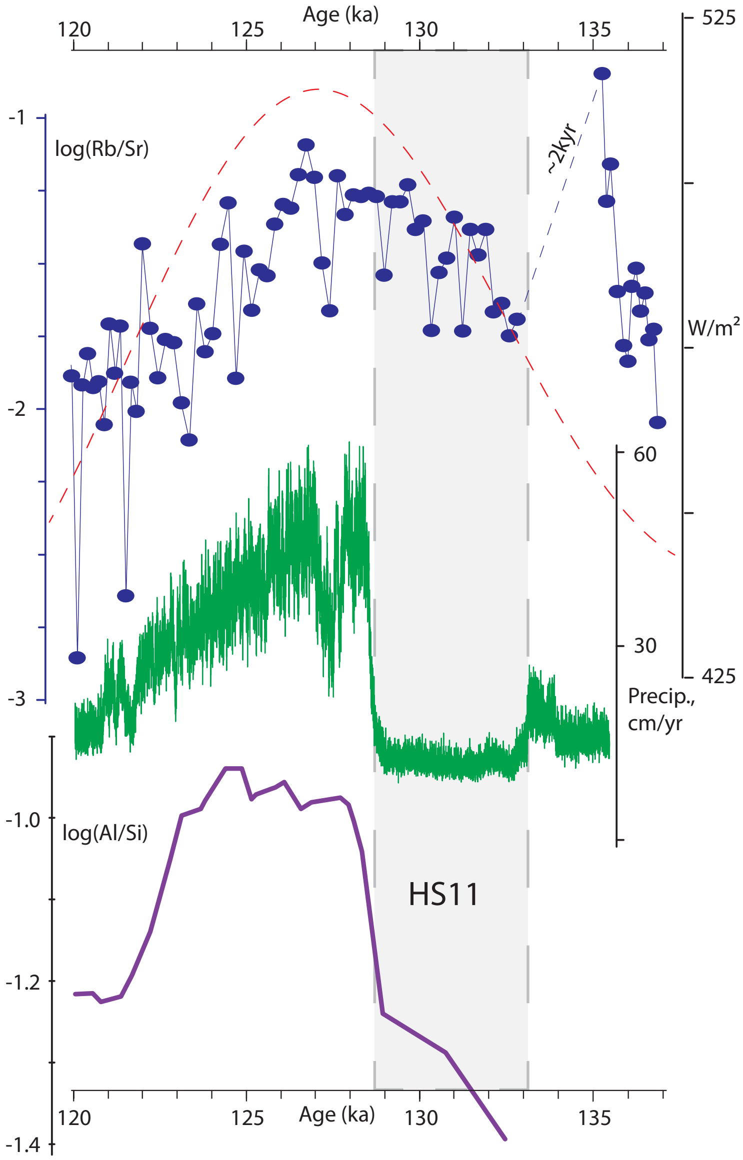

317

Figure 5: Paleoclimate conditions through the penultimate deglaciation and the previous interglacial. The log(Rb/Sr) timeseries and summer insolation curve is the same as in Fig. 3 (this study). Model simulations for West Sahara precipitation, middle graph (green data), from Menviel et al. (Menviel et al., 2021). Marine core geologic data showing changes in the Al and Si ratio of subtropical West African core GeoB7925-1 (Govin et al., 2014). Gray shading and dashed box indicate the main phase of Heinrich stadial 11 (HS11).

https://doi.org/10.5194/cp-2022-40
Preprint. Discussion started: 13 May 2022

To explain the drought-like conditions during HS11, it has been suggested that deglaciation may have changed AMOC strength leading to variations in the mean annual position of the ITCZ rainfall (Castaneda et al., 2009; Menviel et al., 2021; Mulitza et al., 2008). Weakened AMOC may result in a warmer south than north Atlantic Ocean(Chadwick et al., 2020), displacing the ITCZ and trade winds to the south (Schneider et al., 2014). Shifting the mean annual position of the ITCZ causes the dust-flux records of different marine core sites to vary according to latitude (Jacobel et al., 2016).

A southward shift of the ITCZ over northern Africa may have had a limited drought effect on low-latitude dust sources. Alternatively, northern African sites nearer to 20° N experienced drier conditions during HS11 (Govin et al., 2014) as a consequence of the ITCZ being located farther south during the summer (Menviel et al., 2021). A spring insolation component to the log(Rb/Sr) timeseries of VM 30-40 (**Fig. 5A**) may suggest that some of the terrigenous source areas were in the low latitudes. The monsoon of low latitude Africa is most sensitive to insolation forcing during spring and autumn. This is due to the sun passing over the equator twice a year at each equinox (Berger and Loutre, 1997). Within the low-latitude intertropical zone, two rainy seasons occur in spring and autumn, and the solstices are dry (Verschuren et al., 2009).

Figure 6: Gaussian filter of the log(Rb/Sr) VM 30-40 timeseries (frequency = 0.043, bandwidth = 0.009) compared to astronomical insolation solutions. (A) Mean spring (March 21 – May 21; MAM) insolation at the equator. (B) Mean summer (June 21 – August 21; JJA) at 23° N.

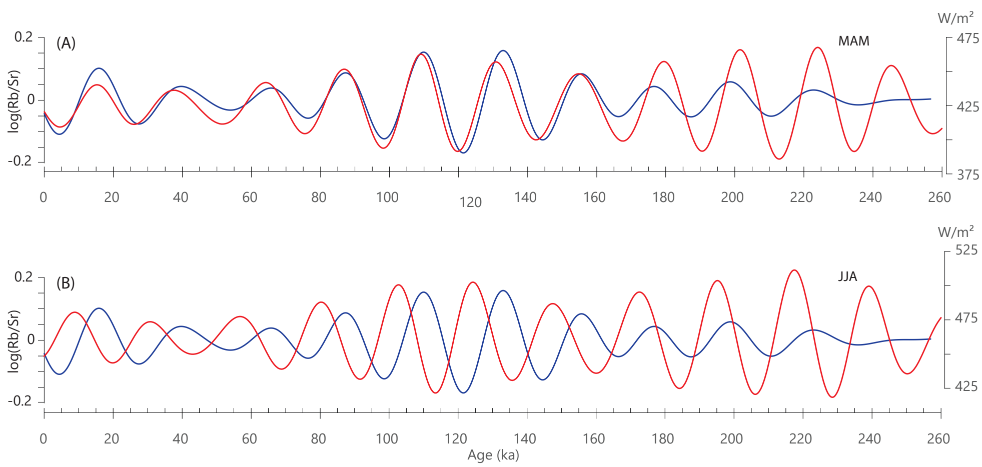

4.3. Possible implications for the West African MSA

The late Pleistocene witnessed the emergence and dispersal of *Homo sapiens* populations across northern and eastern Africa (Hublin et al., 2017; McDougall et al., 2005; Vidal et al., 2022), as well as

https://doi.org/10.5194/cp-2022-40
Preprint. Discussion started: 13 May 2022

genetic divergences at ~80-20 ka across sub-Saharan regions (Lipson et al., 2022). In West Africa, most evidence of late Pleistocene *H. sapiens* is known from MSA sites from a few well-studied localities in Senegal and Mali. Their assemblages include typical artifacts made by bifacial, retouched, and bipolar percussive techniques (Allsworth-Jones, 2021). Artifact assemblages from earlier part of MIS 5 are some of the oldest MSA from West Africa (Douze et al., 2021). The younger part of the sequence is constrained by OSL to about 75-25 ka, yet several of the dates are considered to be only minimum possible ages (Chevrier et al., 2018).

The dissimilarities in the MSA archaeology across western to northern Africa has led some to suggest that a cultural frontier existed between the regions (Chevrier et al., 2018). However, Levallois core reduction is one of the few techniques shared between the West African MSA and lithic assemblages from North Africa and the Sahara (Allsworth-Jones, 2021). During wet/warm phases, Levallois culture may have been transmitted across the frontier, assisted by the expansion of waterways that extended social routes through northern Africa (Drake et al., 2011).

Unlike other studies, we do not find a spurious (Skonieczny et al., 2019) or paleoclimatic (deMenocal, 2004) obliquity component to the African monsoon. Precession, however, may have been primarily responsible for monsoonal changes that impacted MSA cultures. Of the older assemblages, unidirectional Levallois cores of the Falémé Valley (Douze et al., 2021) were recovered from horizons that formed during wet-warm conditions of MIS 5e and the transition to 5d. Younger archaeological sites constrained to MIS 4 and 3 have Levallois debitage patterns that are correlated to warm/wet intervals (Chevrier et al., 2018). Levallois technological characteristics appear to be absent from intervals with low precession-derived insolation associated with the dry-cold phases of MIS 5, 4, and 3 (Douze et al., 2021; Rasse et al., 2020; Schmid et al., 2021; Hawkins et al., 1996).

5. Conclusions

We constructed a new XRF-measured Rb/Sr record for eastern equatorial Atlantic marine core sediments of VM 30-40 and performed spectral coherency analysis that demonstrated a record of climatic precession carried by terrigenous material. However, the largest Rb/Sr ratios of the entire record were observed at glacial maxima of MIS 6 and 2. We also suggest a correlation between climatic precession

https://doi.org/10.5194/cp-2022-40
Preprint. Discussion started: 13 May 2022

cycles and Levallois archaeological patterns. Based on the collected data and interpretations, the main conclusions of the research are summarized as:

- The partitioning of Rb- and Sr-bearing terrigenous fractions of the core appears to be free of successive dissolution cycles caused by obliquity-paced glacial modification of Atlantic bottom waters. This is in contrast to West African marine sediment cores from subtropical latitudes (Skonieczny et al., 2019). However, glacial epochs may be responsible for changes of physical versus chemical weathering on the continent that manifest in the Rb/Sr ratios. Anomalously high Rb/Sr values at MIS 6 and 2 may be a product of this differential weather or glacial bottom water dissolution that preferentially attacked Sr-bearing phases.
- Over the last ~260 kyr, the filtered precession timeseries from the Rb/Sr record show better phase relationships with spring (March, April, May) insolation at the equator as compared to summer (June, July, August) insolation at the northern subtropics. This is unexpected because the largest convectional changes of the West African monsoon are associated with the summer and winter months. However, modern observations document sizable West African dust plumes that emanate from the low latitudes during March and April. A spring moisture signal in the Rb/Sr timeseries may be indicative of turbulence and storminess that accompanies the pre-onset rainy seasons of the West African monsoon. The spring insolation component to the terrigenous record may also suggest that some of the Rb and Sr sources were situated within the low latitudes, where the monsoonal cycle is most sensitive to insolation changes about the equinoxes.
- The Rb/Sr timeseries of early MIS 5e indicates that warm, wet conditions developed in concert with rising insolation and reached a maximum at ~127 ka. Contrastingly, model simulation results and terrigenous proxy data for 20º N (Govin et al., 2014; Menviel et al., 2021) demonstrate a dry HS11 followed by an abrupt increase in rainfall that peaks ~1.4 kyr before the insolation maximum of MIS 5e. These subtropical patterns derived from Northern Hemisphere glacial modification of AMOC that shifted the latitudinal range of the seasonal rainfall belt. We explain the differences by assuming the Rb and Sr had low-latitude source areas that were buffered from AMOC effects because the sources were into the direction of the southward displacement of the ITCZ.

https://doi.org/10.5194/cp-2022-40
Preprint. Discussion started: 13 May 2022

- The precession cycle of isolation was inferred to have modulated moisture change through Middle Stone Age paleoenvironments. Levallois stone artifacts are currently only known from the wetter/warmer phases of the climate cycles through MIS 5, 4 and 3. Because this debitage type is one of the few techniques shared between west and northern Africa, these observations may support previous hypotheses that suggest social networks were enhanced between the regions during times of increased rainfall.

https://doi.org/10.5194/cp-2022-40
Preprint. Discussion started: 13 May 2022

Appendix A

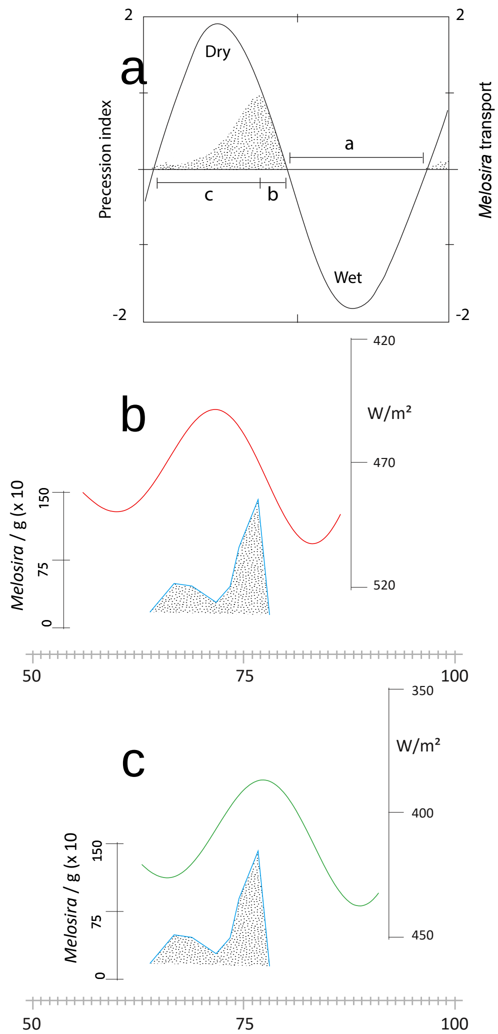

Fig. A1: (**upper panel**) Cartoon of Pokras and Mix (Pokras and Mix, 1987) to show how diatom input (*Melosira*) to the marine realm my predate maximum aridity over a precession cycle of insolation. In time a, lake level is high and diatomite cannot be eroded. In time b, lower lake level and significant erosion occurs, which supplies the marine site with ample diatomite. By time c, diatomite sources have been depleted during continued fall in lake level. Smaller areas of sediment are exposed and the formation of soils or crusts on dry lake beds inhibit further aeolian transport despite ongoing aridity. (**middle panel**) Alignment of the Pokras and Mix (Pokras and Mix, 1987) diatom maximum at ~77 ka to the June solstice insolation minimum center between ~60-83 ka (Laskar et al., 2004). (**lower panel**) Alignment of the Pokras and Mix (Pokras and Mix, 1987) diatom maximum at ~77 ka to the March equinox insolation minimum center between ~66-89 ka (Laskar et al., 2004). Note the insolation scales are inverted.

Sample availability

VM 30-40 is available for inspection at the Lamont-Doherty Earth Observatory Core Repository

Supplement link

A link to the XRF data used for this study will be provided by Copernicus

Author contribution

The research paper was conceived and written by the primary author. The other authors contributed to the manuscript by reviewing and editing. The primary author conducted the formal analysis and investigations, with respect to the geological and paleoclimatic implications. The secondary and tertiary authors were responsible for the curation and collection of the XRF measurements and the first-order interpretation of these data.

Competing interests

The authors declare that they have no conflict of interest

Acknowledgements

We thank Maureen Raymo and Nichole Anest for access to the Lamont-Doherty Core Repository. Paul Olsen, Michael Kaplan, and Dallas Abbott helped organize the research cohort from which this work grew. Funding for this work was contributed by NSF award #1818805 (Lepre) and the NSF REU award # 1757602 (Abbott and Kaplan) to Columbia University.

References

Adkins, J., deMenocal, P., Eshel, G., 2006. The "African humid period" and the record of marine upwelling from excess ^{230}Th in Ocean Drilling Program Hole 658C: Th NORMALIZED FLUXES OFF NORTH AFRICA. Paleoceanography 21. https://doi.org/10.1029/2005PA001200

Allsworth-Jones, P., 2021. The West African Stone Age, in: Oxford Research Encyclopedia of Anthropology. Oxford University Press. https://doi.org/10.1093/acrefore/9780190854584.013.55

Armitage, S.J., Bristow, C.S., Drake, N.A., 2015. West African monsoon dynamics inferred from abrupt fluctuations of Lake Mega-Chad. Proc Natl Acad Sci USA 112, 8543–8548. https://doi.org/10.1073/pnas.1417655112

Balsam, W.L., Otto-Bliesner, B.L., Deaton, B.C., 1995. Modern and Last Glacial Maximum eolian sedimentation patterns in the Atlantic Ocean interpreted from sediment iron oxide content. Paleoceanography 10, 493–507. https://doi.org/10.1029/95PA00421

Barkley, A.E., Prospero, J.M., Mahowald, N., Hamilton, D.S., Popendorf, K.J., Oehlert, A.M., Pourmand, A., Gatineau, A., Panechou-Pulcherie, K., Blackwelder, P., Gaston, C.J., 2019. African biomass burning is a substantial source of phosphorus deposition to the Amazon, Tropical Atlantic Ocean, and Southern Ocean. Proc Natl Acad Sci USA 116, 16216–16221. https://doi.org/10.1073/pnas.1906091116

Berger, A., Loutre, M.F., 1997. Intertropical Latitudes and Precessional and Half-Precessional Cycles. Science 278, 1476–1478. https://doi.org/10.1126/science.278.5342.1476

Berger, A., Loutre, M.F., Mélice, J.L., 2006. Equatorial insolation: from precession harmonics to eccentricity frequencies. Clim. Past 7.

Berner, N., Trauth, M.H., Holschneider, M., 2022. Bayesian inference about Plio-Pleistocene climate transitions in Africa. Quaternary Science Reviews 277, 107287. https://doi.org/10.1016/j.quascirev.2021.107287

Blanchet, C.L., Osborne, A.H., Tjallingii, R., Ehrmann, W., Friedrich, T., Timmermann, A., Brückmann, W., Frank, M., 2021. Drivers of river reactivation in North Africa during the last glacial cycle. Nat. Geosci. 14, 97–103. https://doi.org/10.1038/s41561-020-00671-3

Bloemendal, J., deMenocal, P., 1989. Evidence for a change in the periodicity of tropical climate cycles at 2.4 Myr from whole-core magnetic susceptibility measurements. Nature 342, 897–900. https://doi.org/10.1038/342897a0

Bloemendal, J., Lamb, B., King, J., 1988. Paleoenvironmental implications of rock-magnetic properties of Late Quaternary sediment cores from the eastern equatorial Atlantic. Paleoceanography 3, 61–87. https://doi.org/10.1029/PA003i001p00061

Blum, J.D., Erel, I.Y., Brown, K., 1994. 878r/S6Srratios of Sierra Nevada stream waters: Implications for relative mineral weathering rates 7.

Blum, J.D., Erel, Y., 1997. Rb□Sr isotope systematics of a granitic soil chronosequence: The importance of biotite weathering. Geochimica et Cosmochimica Acta 61, 3193–3204. https://doi.org/10.1016/S0016-7037(97)00148-8

Bosmans, J.H.C., Hilgen, F.J., Tuenter, E., Lourens, L.J., 2015. Obliquity forcing of low-latitude climate. Clim. Past 11, 1335–1346. https://doi.org/10.5194/cp-11-1335-2015

Bozzano, G., Kuhlmann, H., Alonso, B., 2002. Storminess control over African dust input to the Moroccan Atlantic margin (NW Africa) at the time of maxima boreal summer insolation: a record of the last 220 kyr. Palaeogeography, Palaeoclimatology, Palaeoecology 183, 155–168. https://doi.org/10.1016/S0031-0182(01)00466-7

Bradtmiller, L.I., Anderson, R.F., Fleisher, M.Q., Burckle, L.H., 2007. Opal burial in the equatorial Atlantic Ocean over the last 30 ka: Implications for glacial-interglacial changes in the ocean silicon cycle: EQUATORIAL ATLANTIC OPAL BURIAL. Paleoceanography 22, n/a-n/a. https://doi.org/10.1029/2007PA001443

Castaneda, I.S., Mulitza, S., Schefuss, E., Lopes dos Santos, R.A., Sinninghe Damste, J.S., Schouten, S., 2009. Wet phases in the Sahara/Sahel region and human migration patterns in North Africa. Proceedings of the National Academy of Sciences 106, 20159–20163. https://doi.org/10.1073/pnas.0905771106

Chadwick, M., Allen, C.S., Sime, L.C., Hillenbrand, C.-D., 2020. Analysing the timing of peak warming and minimum winter sea-ice extent in the Southern Ocean during MIS 5e. Quaternary Science Reviews 229, 106134. https://doi.org/10.1016/j.quascirev.2019.106134

Chen, J., An, Z., Head, J., 1999. Variation of Rb/Sr Ratios in the Loess-Paleosol Sequences of Central China during the Last 130,000 Years and Their Implications for Monsoon Paleoclimatology. Quat. res. 51, 215–219. https://doi.org/10.1006/qres.1999.2038

Chevrier, B., Huysecom, É., Soriano, S., Rasse, M., Lespez, L., Lebrun, B., Tribolo, C., 2018. Between continuity and discontinuity: An overview of the West African Paleolithic over the last 200,000 years. Quaternary International 466, 3–22. https://doi.org/10.1016/j.quaint.2017.11.027

Clement, A.C., Hall, A., Broccoli, A.J., 2004. The importance of precessional signals in the tropical climate. Climate Dynamics 22, 327–341. https://doi.org/10.1007/s00382-003-0375-8

Cole, J.M., Goldstein, S.L., deMenocal, P.B., Hemming, S.R., Grousset, F.E., 2009. Contrasting compositions of Saharan dust in the eastern Atlantic Ocean during the last deglaciation and African Humid Period. Earth and Planetary Science Letters 278, 257–266. https://doi.org/10.1016/j.epsl.2008.12.011

de Boer, B., Peters, M., Lourens, L.J., 2020. The transient impact of the African monsoon on Plio-Pleistocene Mediterranean sediments (preprint). Feedback and Forcing/Marine Archives/Pleistocene. https://doi.org/10.5194/cp-2020-97

de Menocal, P.B., 2015. End of the African Humid Period. Nature Geosci 8, 86–87. https://doi.org/10.1038/ngeo2355

deMenocal, P.B., 2004. African climate change and faunal evolution during the Pliocene–Pleistocene. Earth and Planetary Science Letters 220, 3–24. https://doi.org/10.1016/S0012-821X(04)00003-2

deMenocal, P.B., Ruddiman, W.F., Pokras, E.M., 1993. Influences of High- and Low-Latitude Processes on African Terrestrial Climate: Pleistocene Eolian Records from Equatorial Atlantic Ocean Drilling Program Site 663. Paleoceanography 8, 209–242. https://doi.org/10.1029/93PA02688

Douze, K., Lespez, L., Rasse, M., Tribolo, C., Garnier, A., Lebrun, B., Mercier, N., Ndiaye, M., Chevrier, B., Huysecom, E., 2021. A West African Middle Stone Age site dated to the beginning of MIS 5: Archaeology, chronology, and paleoenvironment of the Ravin Blanc I (eastern Senegal). Journal of Human Evolution 154, 102952. https://doi.org/10.1016/j.jhevol.2021.102952

Drake, N.A., Blench, R.M., Armitage, S.J., Bristow, C.S., White, K.H., 2011. Ancient watercourses and biogeography of the Sahara explain the peopling of the desert. Proceedings of the National Academy of Sciences 108, 458–462. https://doi.org/10.1073/pnas.1012231108

Dupont, L., 2011. Orbital scale vegetation change in Africa. Quaternary Science Reviews 30, 3589–3602. https://doi.org/10.1016/j.quascirev.2011.09.019

Formenti, P., Caquineau, S., Chevaillier, S., Klaver, A., Desboeufs, K., Rajot, J.L., Belin, S., Briois, V., 2014. Dominance of goethite over hematite in iron oxides of mineral dust from Western Africa:

Quantitative partitioning by X-ray absorption spectroscopy. J. Geophys. Res. Atmos. 119, 12,740-12,754. https://doi.org/10.1002/2014JD021668
Gasse, F., 2000. Hydrological changes in the African tropics since the Last Glacial Maximum. Quaternary Science Reviews 19, 189–211. https://doi.org/10.1016/S0277-3791(99)00061-X
Govin, A., Capron, E., Tzedakis, P.C., Verheyden, S., Ghaleb, B., Hillaire-Marcel, C., St-Onge, G., Stoner, J.S., Bassinot, F., Bazin, L., Blunier, T., Combourieu-Nebout, N., El Ouahabi, A., Genty, D., Gersonde, R., Jimenez-Amat, P., Landais, A., Martrat, B., Masson-Delmotte, V., Parrenin, F., Seidenkrantz, M.-S., Veres, D., Waelbroeck, C., Zahn, R., 2015. Sequence of events from the onset to the demise of the Last Interglacial: Evaluating strengths and limitations of chronologies used in climatic archives. Quaternary Science Reviews 129, 1–36. https://doi.org/10.1016/j.quascirev.2015.09.018
Govin, A., Varma, V., Prange, M., 2014. Astronomically forced variations in western African rainfall (21°N-20°S) during the Last Interglacial period: Govin et al.: Last Interglacial African precipitation. Geophys. Res. Lett. 41, 2117–2125. https://doi.org/10.1002/2013GL058999
Grant, K.M., Amarathunga, U., Amies, J.D., Hu, P., Qian, Y., Penny, T., Rodriguez-Sanz, L., Zhao, X., Heslop, D., Liebrand, D., Hennekam, R., Westerhold, T., Gilmore, S., Lourens, L.J., Roberts, A.P., Rohling, E.J., 2022. Organic carbon burial in Mediterranean sapropels intensified during Green Sahara Periods since 3.2 Myr ago. Commun Earth Environ 3, 11. https://doi.org/10.1038/s43247-021-00339-9
Heinrich, H., Schmidt, C., Ziemen, F., Mikolajewicz, U., Roettig, C.-B., 2021. Massive deposition of Sahelian dust on the Canary Island Lanzarote during North Atlantic Heinrich Events. Quat. res. 1–16. https://doi.org/10.1017/qua.2020.100
Hemming, S.R., 2007. Terrigenous Sediments, in: Encyclopedia of Quaternary Science. Elsevier, Oxford, UK, pp. 1776–1785.
Hodell, D., Lourens, L., Crowhurst, S., Konijnendijk, T., Tjallingii, R., Jiménez-Espejo, F., Skinner, L., Tzedakis, P.C., Abrantes, F., Acton, G.D., Alvarez Zarikian, C.A., Bahr, A., Balestra, B., Barranco, E.L., Carrara, G., Ducassou, E., Flood, R.D., Flores, J.-A., Furota, S., Grimalt, J., Grunert, P., Hernández-Molina, J., Kim, J.K., Krissek, L.A., Kuroda, J., Li, B., Lofi, J., Margari, V., Martrat, B., Miller, M.D., Nanayama, F., Nishida, N., Richter, C., Rodrigues, T., Rodríguez-Tovar, F.J., Roque, A.C.F., Sanchez Goñi, M.F., Sierro Sánchez, F.J., Singh, A.D., Sloss, C.R., Stow, D.A.V., Takashimizu, Y., Tzanova, A., Voelker, A., Xuan, C., Williams, T., 2015. A reference time scale for Site U1385 (Shackleton Site) on the SW Iberian Margin. Global and Planetary Change 133, 49–64. https://doi.org/10.1016/j.gloplacha.2015.07.002
Hooghiemstra, H., Lézine, A.-M., Leroy, S.A.G., Dupont, L., Marret, F., 2006. Late Quaternary palynology in marine sediments: A synthesis of the understanding of pollen distribution patterns in the NW African setting. Quaternary International 148, 29–44. https://doi.org/10.1016/j.quaint.2005.11.005
Hublin, J.-J., Ben-Ncer, A., Bailey, S.E., Freidline, S.E., Neubauer, S., Skinner, M.M., Bergmann, I., Le Cabec, A., Benazzi, S., Harvati, K., Gunz, P., 2017. New fossils from Jebel Irhoud, Morocco and the pan-African origin of Homo sapiens. Nature 546, 289–292. https://doi.org/10.1038/nature22336
Imbrie et al., J., 1984. The orbital theory of Pleistocene climate: support from a revised chronology of the marine δ18O record.
Jacobel, A.W., McManus, J.F., Anderson, R.F., Winckler, G., 2016. Large deglacial shifts of the Pacific Intertropical Convergence Zone. Nat Commun 7, 10449. https://doi.org/10.1038/ncomms10449
Janicot, S., Lafore, J.-P., Thorncroft, C., 2011. THE WEST AFRICAN MONSOON 25.
Janzen, A., Bataille, C., Copeland, S.R., Quinn, R.L., Ambrose, S.H., Reed, D., Hamilton, M., Grimes, V., Richards, M.P., le Roux, P., Roberts, P., 2020. Spatial variation in bioavailable strontium isotope ratios (87Sr/86Sr) in Kenya and northern Tanzania: Implications for ecology, paleoanthropology, and archaeology. Palaeogeography, Palaeoclimatology, Palaeoecology 109957. https://doi.org/10.1016/j.palaeo.2020.109957
Jewell, A.M., Drake, N., Crocker, A.J., Bakker, N.L., Kunkelova, T., Bristow, C.S., Cooper, M.J., Milton, J.A., Breeze, P.S., Wilson, P.A., 2021. Three North African dust source areas and their geochemical fingerprint. Earth and Planetary Science Letters 554, 116645. https://doi.org/10.1016/j.epsl.2020.116645

Jung, S.J.A., Davies, G.R., Ganssen, G.M., Kroon, D., 2004. Stepwise Holocene aridification in NE Africa deduced from dust-borne radiogenic isotope records. Earth and Planetary Science Letters 221, 27–37. https://doi.org/10.1016/S0012-821X(04)00095-0
Kaboth-Bahr, S., Gosling, W.D., Vogelsang, R., Bahr, A., Scerri, E.M.L., Asrat, A., Cohen, A.S., Düsing, W., Foerster, V., Lamb, H.F., Maslin, M.A., Roberts, H.M., Schäbitz, F., Trauth, M.H., 2021. Paleo-ENSO influence on African environments and early modern humans. Proc Natl Acad Sci USA 118, e2018277118. https://doi.org/10.1073/pnas.2018277118
Kelly, E.F., Chadwick, O.A., Hilinski, T.E., 1998. The effect of plants on mineral weathering. Biogeochemistry 42, 21–53.
Kim, S.-J., Crowley, T.J., Erickson, D.J., Govindasamy, B., Duffy, P.B., Lee, B.Y., 2008. High-resolution climate simulation of the last glacial maximum. Clim Dyn 31, 1–16. https://doi.org/10.1007/s00382-007-0332-z
Koch, P.L., Halliday, A.N., Walter, L.M., Stearley, R.F., Huston, T.J., Smith, G.R., 1992. Sr isotopic composition of hydroxyapatite from recent and fossil salmon: the record of lifetime migration and diagenesis. Earth and Planetary Science Letters 108, 277–287. https://doi.org/10.1016/0012-821X(92)90028-T
Kukla, G.J., Bender, M.L., de Beaulieu, J.-L., Bond, G., Broecker, W.S., Cleveringa, P., Gavin, J.E., Herbert, T.D., Imbrie, J., Jouzel, J., Keigwin, L.D., Knudsen, K.-L., McManus, J.F., Merkt, J., Muhs, D.R., Müller, H., Poore, R.Z., Porter, S.C., Seret, G., Shackleton, N.J., Turner, C., Tzedakis, P.C., Winograd, I.J., 2002. Last Interglacial Climates. Quat. res. 58, 2–13. https://doi.org/10.1006/qres.2001.2316
Kutzbach, J.E., Liu, Z., 1997. Response of the African Monsoon to Orbital Forcing and Ocean Feedbacks in the Middle Holocene. Science 278, 440–443. https://doi.org/10.1126/science.278.5337.440
Laskar, J., Robutel, P., Joutel, F., Gastineau, M., Correia, A.C.M., Levrard, B., 2004. A long-term numerical solution for the insolation quantities of the Earth. Astronomy & Astrophysics 428, 261–285. https://doi.org/10.1051/0004-6361:20041335
Lepre, C.J., Quinn, R.L., 2022. Aridification and orbital forcing of eastern African climate during the Plio-Pleistocene. Global and Planetary Change 208, 103684. https://doi.org/10.1016/j.gloplacha.2021.103684
Leroy, S., Dupont, L., 1994. Development of vegetation and continental aridity in northwestern Africa during the Late Pliocene: the pollen record of ODP site 658. Palaeogeography, Palaeoclimatology, Palaeoecology 109, 295–316. https://doi.org/10.1016/0031-0182(94)90181-3
Lespez, L., Rasse, M., Drézen, Y.L., Tribolo, C., Huysecom, E., Ballouche, A., 2008. L'évolution hydromorphologique de la vallée du Yamé (Pays Dogon, Mali) : signal climatique et hydrosystème continental en Afrique de l'Ouest entre 50 et 4 ka cal. BP. geomorphologie 14, 170–185. https://doi.org/10.4000/geomorphologie.7053
Lézine, A.-M., Casanova, J., 1991. Correlated oceanic and continental records demonstrate past climate and hydrology of North Africa (0-140 ka). Geol 19, 307. https://doi.org/10.1130/0091-7613(1991)019<0307:COACRD>2.3.CO;2
Lipson, M., Sawchuk, E.A., Thompson, J.C., Oppenheimer, J., Tryon, C.A., Ranhorn, K.L., de Luna, K.M., Sirak, K.A., Olalde, I., Ambrose, S.H., Arthur, J.W., Arthur, K.J.W., Ayodo, G., Bertacchi, A., Cerezo-Román, J.I., Culleton, B.J., Curtis, M.C., Davis, J., Gidna, A.O., Hanson, A., Kaliba, P., Katongo, M., Kwekason, A., Laird, M.F., Lewis, J., Mabulla, A.Z.P., Mapemba, F., Morris, A., Mudenda, G., Mwafulirwa, R., Mwangomba, D., Ndiema, E., Ogola, C., Schilt, F., Willoughby, P.R., Wright, D.K., Zipkin, A., Pinhasi, R., Kennett, D.J., Manthi, F.K., Rohland, N., Patterson, N., Reich, D., Prendergast, M.E., 2022. Ancient DNA and deep population structure in sub-Saharan African foragers. Nature. https://doi.org/10.1038/s41586-022-04430-9
Lisiecki, L.E., Raymo, M.E., 2005. A Pliocene-Pleistocene stack of 57 globally distributed benthic $\delta^{18}O$ records: PLIOCENE-PLEISTOCENE BENTHIC STACK. Paleoceanography 20, n/a-n/a. https://doi.org/10.1029/2004PA001071
Lourens, L.J., Antonarakou, A., Hilgen, F.J., Van Hoof, A.A.M., Vergnaud-Grazzini, C., Zachariasse, W.J., 1996. Evaluation of the Plio-Pleistocene astronomical timescale. Paleoceanography 11, 391–413. https://doi.org/10.1029/96PA01125
Mabbutt, J.A., 1977. Desert landforms. Australian National University Press, Canberra.

https://doi.org/10.5194/cp-2022-40
Preprint. Discussion started: 13 May 2022

Climate of the Past Discussions Open Access EGU

Maher, B.A., Prospero, J.M., Mackie, D., Gaiero, D., Hesse, P.P., Balkanski, Y., 2010. Global connections between aeolian dust, climate and ocean biogeochemistry at the present day and at the last glacial maximum. Earth-Science Reviews 99, 61–97. https://doi.org/10.1016/j.earscirev.2009.12.001

McDougall, I., Brown, F.H., Fleagle, J.G., 2005. Stratigraphic placement and age of modern humans from Kibish, Ethiopia. Nature 433, 733–736. https://doi.org/10.1038/nature03258

McGee, D., deMenocal, P.B., Winckler, G., Stuut, J.B.W., Bradtmiller, L.I., 2013. The magnitude, timing and abruptness of changes in North African dust deposition over the last 20,000yr. Earth and Planetary Science Letters 371–372, 163–176. https://doi.org/10.1016/j.epsl.2013.03.054

McIntyre, A., Ruddiman, W.F., Karlin, K., Mix, A.C., 1989. Surface water response of the equatorial Atlantic Ocean to orbital forcing. Paleoceanography 4, 19–55. https://doi.org/10.1029/PA004i001p00019

Menviel, L., Govin, A., Avenas, A., Meissner, K.J., Grant, K.M., Tzedakis, P.C., 2021. Drivers of the evolution and amplitude of African Humid Periods. Commun Earth Environ 2, 237. https://doi.org/10.1038/s43247-021-00309-1

Moreno, A., Targarona, J., Henderiks, J., Canals, M., Freudenthal, T., Meggers, H., 2001. Orbital forcing of dust supply to the North Canary Basin over the last 250kyr. Quaternary Science Reviews 20, 1327–1339. https://doi.org/10.1016/S0277-3791(00)00184-0

Moreno, T., Querol, X., Castillo, S., Alastuey, A., Cuevas, E., Herrmann, L., Mounkaila, M., Elvira, J., Gibbons, W., 2006. Geochemical variations in aeolian mineral particles from the Sahara–Sahel Dust Corridor. Chemosphere 65, 261–270. https://doi.org/10.1016/j.chemosphere.2006.02.052

Moskowitz, B.M., Reynolds, R.L., Goldstein, H.L., Berquó, T.S., Kokaly, R.F., Bristow, C.S., 2016. Iron oxide minerals in dust-source sediments from the Bodélé Depression, Chad: Implications for radiative properties and Fe bioavailability of dust plumes from the Sahara. Aeolian Research 22, 93–106. https://doi.org/10.1016/j.aeolia.2016.07.001

Mulitza, S., Heslop, D., Pittauerova, D., Fischer, H.W., Meyer, I., Stuut, J.-B., Zabel, M., Mollenhauer, G., Collins, J.A., Kuhnert, H., Schulz, M., 2010. Increase in African dust flux at the onset of commercial agriculture in the Sahel region. Nature 466, 226–228. https://doi.org/10.1038/nature09213

Mulitza, S., Prange, M., Stuut, J.-B., Zabel, M., von Dobeneck, T., Itambi, A.C., Nizou, J., Schulz, M., Wefer, G., 2008. Sahel megadroughts triggered by glacial slowdowns of Atlantic meridional overturning: SAHEL DROUGHT AND ATLANTIC OVERTURNING. Paleoceanography 23, n/a-n/a. https://doi.org/10.1029/2008PA001637

Nicholson, S.E., 2018. Climate of the Sahel and West Africa, in: Oxford Research Encyclopedia of Climate Science. Oxford University Press. https://doi.org/10.1093/acrefore/9780190228620.013.510

Oldfield, F., Chiverrell, R.C., Lyons, R., Williams, E., Shen, Z., Bristow, C., Bloemendal, J., Torrent, J., Boyle, J.F., 2014. Discriminating dusts and dusts sources using magnetic properties and hematite:Goethite ratios of surface materials and dust from North Africa, the Atlantic and Barbados. Aeolian Research 13, 91–104. https://doi.org/10.1016/j.aeolia.2014.03.010

Oppo, D.W., Fairbanks, R.G., 1987. Variability in the deep and intermediate water circulation of the Atlantic Ocean during the past 25,000 years: Northern Hemisphere modulation of the Southern Ocean 15.

Palchan, D., Torfstein, A., 2019. A drop in Sahara dust fluxes records the northern limits of the African Humid Period. Nat Commun 10, 3803. https://doi.org/10.1038/s41467-019-11701-z

Pokras, E.M., 1987. Diatom record of Late Quaternary climatic change in the eastern equatorial Atlantic and tropical Africa. Paleoceanography 2, 273–286. https://doi.org/10.1029/PA002i003p00273

Pokras, E.M., Mix, A.C., 1987. Earth's precession cycle and Quaternary climatic change in tropical Africa. Nature 326, 486–487. https://doi.org/10.1038/326486a0

Pokras, E.M., Mix, A.C., 1985. Eolian Evidence for Spatial Variability of Late Quaternary Climates in Tropical Africa. Quat. res. 24, 137–149. https://doi.org/10.1016/0033-5894(85)90001-8

Prell, W.L., Kutzbach, J.E., 1987. Monsoon variability over the past 150,000 years. Journal of Geophysical Research 92, 8411. https://doi.org/10.1029/JD092iD07p08411

Prospero, J.M., Barkley, A.E., Gaston, C.J., Gatineau, A., Campos y Sansano, A., Panechou, K., 2020. Characterizing and Quantifying African Dust Transport and Deposition to South America: Implications for the Phosphorus Budget in the Amazon Basin. Global Biogeochemical Cycles 34. https://doi.org/10.1029/2020GB006536

Prospero, J.M., Collard, F.-X., Molinié, J., Jeannot, A., 2014. Characterizing the annual cycle of African dust transport to the Caribbean Basin and South America and its impact on the environment and air quality: African dust transport to South America. Global Biogeochem. Cycles 28, 757–773. https://doi.org/10.1002/2013GB004802

Prospero, J.M., Ginoux, P., Torres, O., Nicholson, S.E., Gill, T.E., 2002. ENVIRONMENTAL CHARACTERIZATION OF GLOBAL SOURCES OF ATMOSPHERIC SOIL DUST IDENTIFIED WITH THE NIMBUS 7 TOTAL OZONE MAPPING SPECTROMETER (TOMS) ABSORBING AEROSOL PRODUCT: GLOBAL SOURCES OF ATMOSPHERIC SOIL DUST. Rev. Geophys. 40, 2-1-2–31. https://doi.org/10.1029/2000RG000095

Prospero, J.M., Glaccum, R.A., Nees, R.T., 1981. Atmospheric transport of soil dust from Africa to South America. Nature 289, 570–572. https://doi.org/10.1038/289570a0

Rasse, M., Lespez, L., Lebrun, B., Tribolo, C., Chevrier, B., Douze, K., Garnier, A., Davidoux, S., Hadjas, I., Ollier, C., Camara, A., Ndiaye, M., Huysecom, E., 2020. Synthèse morpho-sédimentaire et occurences archéologiques dans la vallée de la Falémé (de 80 à 5 ka ; Sénégal oriental) : mise en évidence d'une permanence des occupations à la transition Pléistocène-Holocène. quaternaire 71–88. https://doi.org/10.4000/quaternaire.13181

Rossignol-Strick, M., 1985. Mediterranean Quaternary sapropels, an immediate response of the African monsoon to variation of insolation. Palaeogeography, Palaeoclimatology, Palaeoecology 49, 237–263. https://doi.org/10.1016/0031-0182(85)90056-2

Rowland, G.H., Robinson, L.F., Hendry, K.R., Ng, H.C., McGee, D., McManus, J.F., 2021. The Spatial Distribution of Aeolian Dust and Terrigenous Fluxes in the Tropical Atlantic Ocean Since the Last Glacial Maximum. Paleoceanogr Paleoclimatol 36. https://doi.org/10.1029/2020PA004148

Sarnthein, M., Winn, K., Jung, S.J.A., Duplessy, J.-C., Labeyrie, L., Erlenkeuser, H., Ganssen, G., 1994. Changes in East Atlantic Deepwater Circulation over the last 30,000 years: Eight time slice reconstructions. Paleoceanography 9, 209–267. https://doi.org/10.1029/93PA03301

Scheuvens, D., Schütz, L., Kandler, K., Ebert, M., Weinbruch, S., 2013. Bulk composition of northern African dust and its source sediments — A compilation. Earth-Science Reviews 116, 170–194. https://doi.org/10.1016/j.earscirev.2012.08.005

Schmid, V.C., Douze, K., Tribolo, C., Martinez, M.L., Rasse, M., Lespez, L., Lebrun, B., Hérisson, D., Ndiaye, M., Huysecom, E., 2021. Middle Stone Age Bifacial Technology and Pressure Flaking at the MIS 3 Site of Toumboura III, Eastern Senegal. Afr Archaeol Rev. https://doi.org/10.1007/s10437-021-09463-5

Schneider, T., Bischoff, T., Haug, G.H., 2014. Migrations and dynamics of the intertropical convergence zone. Nature 513, 45–53. https://doi.org/10.1038/nature13636

Schwanghart, W., Schütt, B., 2008. Meteorological causes of Harmattan dust in West Africa. Geomorphology 95, 412–428. https://doi.org/10.1016/j.geomorph.2007.07.002

Shanahan, T.M., McKay, N.P., Hughen, K.A., Overpeck, J.T., Otto-Bliesner, B., Heil, C.W., King, J., Scholz, C.A., Peck, J., 2015. The time-transgressive termination of the African Humid Period. Nature Geosci 8, 140–144. https://doi.org/10.1038/ngeo2329

Short, D.A., Mengel, J.G., 1986. Tropical climatic phase lags and Earth's precession cycle. Nature 323, 48–50. https://doi.org/10.1038/323048a0

Skonieczny, C., McGee, D., Winckler, G., Bory, A., Bradtmiller, L.I., Kinsley, C.W., Polissar, P.J., De Pol-Holz, R., Rossignol, L., Malaizé, B., 2019. Monsoon-driven Saharan dust variability over the past 240,000 years. Sci. Adv. 5, eaav1887. https://doi.org/10.1126/sciadv.aav1887

Stuut, J.-B., 2005. Provenance of present-day eolian dust collected off NW Africa. J. Geophys. Res. 110, D04202. https://doi.org/10.1029/2004JD005161

Sultan, B., Janicot, S., 2003. The West African Monsoon Dynamics. Part II: The "Preonset" and "Onset" of the Summer Monsoon. J. Climate 16, 3407–3427. https://doi.org/10.1175/1520-0442(2003)016<3407:TWAMDP>2.0.CO;2

Swap, R., Garstang, M., Greco, S., Talbot, R., Kallberg, P., 1992. Saharan dust in the Amazon Basin. Tellus B 44, 133–149. https://doi.org/10.1034/j.1600-0889.1992.t01-1-00005.x

Tiedemann, R., Sarnthein, M., Shackleton, N.J., 1994. Astronomic timescale for the Pliocene Atlantic $\delta^{18}O$ and dust flux records of Ocean Drilling Program Site 659. Paleoceanography 9, 619–638. https://doi.org/10.1029/94PA00208

Tisserand, A., Malaizé, B., Jullien, E., Zaragosi, S., Charlier, K., Grousset, F., 2009. African monsoon enhancement during the penultimate glacial period (MIS 6.5 ~ 170 ka) and its atmospheric impact: GLACIAL AFRICAN MONSOON AND ITCZ. Paleoceanography 24, n/a-n/a. https://doi.org/10.1029/2008PA001630

Trauth, M.H., Asrat, A., Berner, N., Bibi, F., Foerster, V., Grove, M., Kaboth-Bahr, S., Maslin, M.A., Mudelsee, M., Schäbitz, F., 2021. Northern Hemisphere Glaciation, African climate and human evolution. Quaternary Science Reviews 268, 107095. https://doi.org/10.1016/j.quascirev.2021.107095

Trauth, M.H., Larrasoaña, J.C., Mudelsee, M., 2009. Trends, rhythms and events in Plio-Pleistocene African climate. Quaternary Science Reviews 28, 399–411. https://doi.org/10.1016/j.quascirev.2008.11.003

Tuenter, E., Weber, S.L., Hilgen, F.J., Lourens, L.J., 2003. The response of the African summer monsoon to remote and local forcing due to precession and obliquity. Global and Planetary Change 36, 219–235. https://doi.org/10.1016/S0921-8181(02)00196-0

van der Lubbe, H.J.L., Hall, I.R., Barker, S., Hemming, S.R., Baars, T.F., Starr, A., Just, J., Backeberg, B.C., Joordens, J.C.A., 2021. Indo-Pacific Walker circulation drove Pleistocene African aridification. Nature 598, 618–623. https://doi.org/10.1038/s41586-021-03896-3

Verardo, D.J., Mcintyre, A., 1994. Production and destruction: Control of biogenous sedimentation in the tropical Atlantic 0_300,000 years B.P. Paleoceanography 9, 63–86.

Verschuren, D., Sinninghe Damsté, J.S., Moernaut, J., Kristen, I., Blaauw, M., Fagot, M., Haug, G.H., CHALLACEA project members, 2009. Half-precessional dynamics of monsoon rainfall near the East African Equator. Nature 462, 637–641. https://doi.org/10.1038/nature08520

Vidal, C.M., Lane, C.S., Asrat, A., Barfod, D.N., Mark, D.F., Tomlinson, E.L., Tadesse, A.Z., Yirgu, G., Deino, A., Hutchison, W., Mounier, A., Oppenheimer, C., 2022. Age of the oldest known Homo sapiens from eastern Africa. Nature 601, 579–583. https://doi.org/10.1038/s41586-021-04275-8

Washington, R., Todd, M.C., Engelstaedter, S., Mbainayel, S., Mitchell, F., 2006. Dust and the low-level circulation over the Bodélé Depression, Chad: Observations from BoDEx 2005. J. Geophys. Res. 111, D03201. https://doi.org/10.1029/2005JD006502

Weltje, G.J., Tjallingii, R., 2008. Calibration of XRF core scanners for quantitative geochemical logging of sediment cores: Theory and application. Earth and Planetary Science Letters 274, 423–438. https://doi.org/10.1016/j.epsl.2008.07.054

White, A.F., Bullen, T.D., Schulz, M.S., Blum, A.E., Huntington, T.G., Peters, N.E., 2001. Differential rates of feldspar weathering in granitic regoliths. Geochimica et Cosmochimica Acta 65, 847–869. https://doi.org/10.1016/S0016-7037(00)00577-9

Yuan, T., Yu, H., Chin, M., Remer, L.A., McGee, D., Evan, A., 2020. Anthropogenic Decline of African Dust: Insights From the Holocene Records and Beyond. Geophys. Res. Lett. 47. https://doi.org/10.1029/2020GL089711

Zeeden, C., Meyers, S.R., Hilgen, F.J., Lourens, L.J., Laskar, J., 2019. Time scale evaluation and the quantification of obliquity forcing. Quaternary Science Reviews 209, 100–113. https://doi.org/10.1016/j.quascirev.2019.01.018